[11] Multidimensional Heteronuclear Nuclear Magnetic Resonance of Proteins

By G. MARIUS CLORE and ANGELA M. GRONENBORN

Introduction

The principal source of geometric information used to solve three-dimensional (3D) structures of proteins by nuclear magnetic resonance (NMR) resides in short (<5 Å) approximate interproton distance restraints derived from nuclear Overhauser enhancement (NOE) measurements.[1] To extract this information it is essential first to assign completely the ^{1}H spectrum of the protein in question and then to assign as many structurally useful NOE interactions as possible. The larger the number of NOE restraints, the higher the precision and accuracy of the resulting structures.[2,3] Indeed, with current state-of-the-art methodology it is now possible to obtain protein NMR structures at a precision and accuracy comparable to 2 Å resolution crystal structures.[2,4]

For proteins less than about 100 residues, conventional homonuclear two-dimensional (2D) NMR methods can be applied with a considerable degree of success.[1] Specifically, a combination of 2D correlation spectroscopy (COSY) and/or homonuclear Hartmann–Hahn spectroscopy (HOHAHA) to delineate intraresidue connectivities via three-bond ^{1}H–^{1}H *J* couplings, and 2D nuclear Overhauser effect spectroscopy (NOESY) to delineate through-space (<5 Å) sequential connectivities along the polypeptide chain is sufficient to assign sequentially the ^{1}H NMR spectrum of such proteins. Further, by making use of iterative assignment procedures, it is possible to obtain a large number of stereospecific assignments

[1] K. Wüthrich, "NMR of Proteins." Wiley, New York, 1986; G. M. Clore and A. M. Gronenborn, *Protein Eng.* **1,** 275 (1987); R. Kaptein, R. Boelens, R. M. Scheek, and W. F. van Gunsteren, *Biochemistry* **27,** 5389 (1988); G. M. Clore and A. M. Gronenborn, *Crit. Rev. Biochem. Mol. Biol.* **24,** 479 (1989); A. Bax, *Annu. Rev. Biochem.* **58,** 223 (1989); J. L. Markley, this series, Vol. 176, p. 12; K. Wüthrich, *J. Biol. Chem.* **265,** 22059 (1990); A. M. Gronenborn and G. M. Clore, *Anal. Chem.* **62,** 2 (1990).

[2] G. M. Clore and A. M. Gronenborn, *Science* **252,** 1390 (1991); G. M. Clore and A. M. Gronenborn, *Annu. Rev. Biophys. Biophys. Chem.* **21,** 29 (1991).

[3] G. M. Clore, M. A. Robien, and A. M. Gronenborn, *J. Mol. Biol.* in press (1993).

[4] G. M. Clore and A. M. Gronenborn, *J. Mol. Biol.* **221,** 47 (1991); B. Shaanan, A. M. Gronenborn, G. H. Cohen, G. L. Gilliland, B. Veerapandian, D. R. Davies, and G. M. Clore, *Science* **257,** 961 (1992).

of β-methylene and methyl groups and to assign nearly all the structurally useful NOEs present in the spectrum. Indeed, this methodology has been applied with considerable success to proteins as large as *Escherichia coli* and human thioredoxin which have 108 and 105 residues, respectively.[5,6]

As the number of residues and molecular mass increases beyond 100 and 12 kDa, respectively, two main obstacles present themselves which prevent the extension of 2D NMR methods to these systems. First, the increased spectral complexity arising from the presence of a larger number of protons results in extensive chemical shift overlap and degeneracy, rendering the 2D spectra uninterpretable. Second, the rotational correlation time increases with molecular weight, resulting in large ^1H line widths and a concomitant severe decrease in the sensitivity of correlation experiments based on intrinsically small three-bond ^1H–^1H couplings. These obstacles can be overcome by increasing the dimensionality of the spectra to resolve problems associated with spectral overlap and by simultaneously making use of heteronuclear couplings that are larger than the line widths to circumvent limitations in sensitivity.[2] This necessitates the use of uniformly ^{15}N- and/or ^{13}C-labeled protein. In proteins that can be overexpressed in bacterial systems, such labeling can be readily achieved by growing the organism in minimal medium supplemented by $^{15}NH_4Cl$ and/or [$^{13}C_6$]glucose as the sole nitrogen and carbon sources, respectively.

The concept of increasing spectral dimensionality to extract information can perhaps most easily be understood by analogy.[2] Consider for example the *Encyclopaedia Britannica*. In a one-dimensional representation, all the information (i.e., words and sentences arranged in a particular set order) present in the encyclopedia would be condensed into a single line. If this line were expanded to two dimensions in the form of a page, the odd word may be resolved, but the vast majority would still be superimposed on one another. When this page is expanded into a book (i.e., three dimensions) comprising a set number of lines and words per page, as well as a fixed number of pages, some pages may become intelligible, but many words will still lie on top of one another. The final expansion to the multivolume book (i.e., four dimensions) then makes it possible to extract in full all the information present in the individual entries of the encyclopedia.

[5] H. J. Dyson, G. P. Gippert, D. A. Case, A. Holmgren, and P. E. Wright, *Biochemistry* **29,** 4129 (1990).

[6] J. D. Forman-Kay, G. M. Clore, P. T. Wingfield, and A. M. Gronenborn, *Biochemistry* **30,** 2685 (1991).

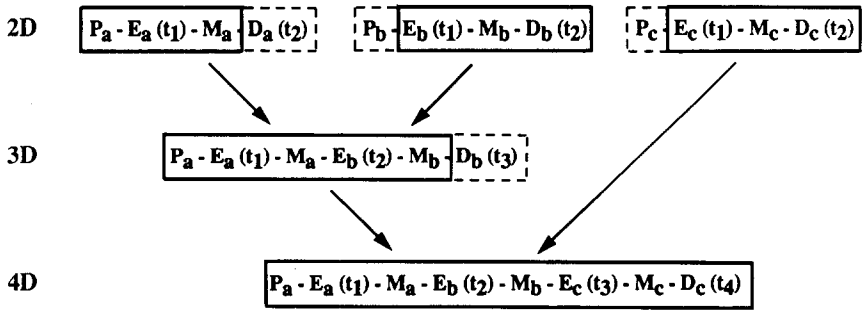

FIG. 1. General representation of pulse sequences used in multidimensional NMR, illustrating the relationship between the basic schemes used to record 2D, 3D, and 4D NMR spectra. Note how 3D and 4D experiments are constructed by the appropriate linear combination of 2D pulse sequences. P, Preparation; E, evolution; M, mixing; and D, detection. In 3D and 4D NMR, the evolution periods are incremented independently.

Application of Multidimensional Heteronuclear Nuclear Magnetic Resonance Spectroscopy to Protein Structure Determination

The design and implementation of higher dimensionality NMR experiments can be carried out by the appropriate combination of 2D NMR experiments, as illustrated schematically in Fig. 1. A 3D experiment is constructed from two 2D pulse schemes by leaving out the detection period of the first experiment and the preparation pulse of the second.[7] This results in a pulse train comprising two independently incremented evolution periods t_1 and t_2, two corresponding mixing periods M_1 and M_2, and a detection period t_3. Similarly, a four-dimensional (4D) experiment is obtained by combining three 2D experiments in an analogous fashion. Thus, conceptually n-dimensional NMR can be conceived as a straightforward extension of 2D NMR. The real challenge, however, of 3D and 4D NMR is 2-fold: first, to ascertain which 2D experiments should be combined to best advantage and, second, to design the pulse sequences in such a way that undesired artifacts, which may severely interfere with the interpretation of the spectra, are removed. This task is far from trivial.

Heteronuclear 3D and 4D NMR experiments exploit a series of large one-bond heteronuclear couplings for magnetization transfer through

[7] C. Griesinger, O. W. Sørensen, and R. R. Ernst, *J. Magn. Reson.* **73,** 574 (1987); H. Oschkinat, C. Griesinger, P. J. Kraulis, O. W. Sørensen, R. R. Ernst, A. M. Gronenborn, and G. M. Clore, *Nature (London)* **332,** 374 (1988).

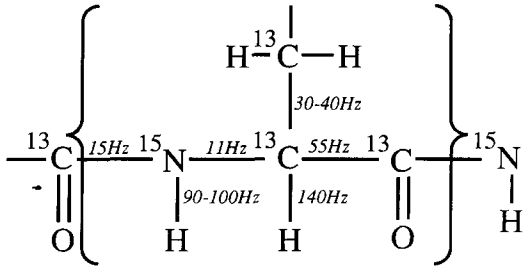

FIG. 2. Summary of one-bond heteronuclear couplings along the polypeptide chain utilized in 3D and 4D NMR experiments.

bonds (Fig. 2). This, together with the fact that the ^{1}H nucleus is always detected, renders these experiments very sensitive. Indeed, high-quality 3D and 4D heteronuclear-edited spectra can easily be obtained on samples of 1–2 m*M* uniformly labeled protein in a time frame that is limited solely by the number of increments that have to be collected for appropriate digitization and the number of phase cycling steps that have to be used to reduce artifacts to an acceptably low level. Typical measurement times are 1 to 3 days for 3D experiments and 2.5 to 5 days for 4D ones. A detailed technical review of heteronuclear multidimensional NMR has been provided by Clore and Gronenborn.[8]

Many of the 3D and 4D experiments are based on heteronuclear editing of ^{1}H–^{1}H experiments so that the general appearance of conventional 2D experiments is preserved and the total number of cross-peaks present is the same as that in the 2D equivalents.[2,8,9] The progression from a 2D spectrum to 3D and 4D heteronuclear-edited spectra is depicted schematically in Fig. 3.[10] Consider, for example, the cross-peaks involving a particular ^{1}H frequency in a 2D NOESY spectrum, a 3D ^{15}N- or ^{13}C-edited NOESY spectrum, and finally a 4D $^{15}N/^{13}C$- or $^{13}C/^{13}C$-edited NOESY spectrum. In the 2D spectrum a series of cross-peaks will be seen from

[8] G. M. Clore and A. M. Gronenborn, *Prog. Nucl. Magn. Reson. Spectrosc.* **23,** 43 (1991).

[9] S. W. Fesik and E. R. P. Zuiderweg, *J. Magn. Reson.* **78,** 588 (1988); D. Marion, L. E. Kay, S. W. Sparks, D. A. Torchia, and A. Bax, *J. Am. Chem. Soc.* **111,** 1515 (1989); D. Marion, P. C. Driscoll, L. E. Kay, P. T. Wingfield, A. Bax, A. M. Gronenborn, and G. M. Clore, *Biochemistry* **29,** 6150 (1989); L. E. Kay, D. Marion, and A. Bax, *J. Magn. Reson.* **84,** 72 (1989); M. Ikura, A. Bax, G. M. Clore, and A. M. Gronenborn, *J. Am. Chem. Soc.* **112,** 9020 (1990); G. M. Clore, A. Bax, P. T. Wingfield, and A. M. Gronenborn, *Biochemistry* **29,** 5671 (1990); M. Ikura, L. E. Kay, R. Tschudin, and A. Bax, *J. Magn. Reson.* **86,** 204 (1990); E. R. P. Zuiderweg, L. P. McIntosh, F. W. Dahlquist, and S. W. Fesik, *J. Magn. Reson.* **86,** 210 (1990).

[10] L. E. Kay, G. M. Clore, A. Bax, and A. M. Gronenborn, *Science* **249,** 411 (1990).

the originating proton frequencies in the F_1 dimension to the single destination ^1H frequency along the F_2 dimension. From the 2D experiment, it is impossible to ascertain whether these NOEs involve only a single destination proton or several destination protons with identical chemical shifts. By spreading the spectrum into a third dimension according to the chemical shift of the heteronucleus attached to the destination proton(s), NOEs involving different destination protons will appear in distinct ^1H–^1H planes of the 3D spectrum. Thus, each interaction is simultaneously labeled by three chemical shift coordinates along three orthogonal axes of the spectrum. The projection of all these planes onto a single plane yields the corresponding 2D spectrum.

For the purposes of sequential assignment, heteronuclear-edited 3D spectra are often sufficient for analysis. However, when the goal of the analysis is to assign NOEs between protons far apart in the sequence, a 3D ^{15}N- or ^{13}C-edited NOESY spectrum will often prove inadequate. This is because the originating protons are only specified by their ^1H chemical shifts, and, more often than not, there are several protons which resonate at the same frequencies. For example, in the case of the 153-residue protein interleukin 1β, there are about 60 protons which resonate in a 0.4 ppm interval between 0.8 and 1.2 ppm. Such ambiguities can then be resolved by spreading out the 3D spectrum still further into a fourth dimension according to the chemical shift of the heteronucleus attached to the originating protons, so that each NOE interaction is simultaneously labeled by four chemical shift coordinates along four orthogonal axes, namely, those of the originating and destination protons and those of the corresponding heteronuclei directly bonded to these protons.[10-12] The result is a 4D spectrum in which each plane of the 3D spectrum constitutes a cube in the 4D spectrum.

For illustration purposes it is also useful to compare the type of information that can be extracted from a very simple system using 2D, 3D, and 4D NMR. Consider a molecule with only two NH and two aliphatic protons in which only one NH proton is close to an aliphatic proton. In addition, the chemical shifts of the NH protons are degenerate, as are those of the aliphatic protons, so that only two resonances are seen in the one-dimensional spectrum. In the 2D NOESY spectrum, an NOE will be observed between the resonance position of the NH protons and the resonance position of the aliphatic protons, but it will be impossible to ascertain which one of the four possible NH–aliphatic proton combina-

[11] G. M. Clore, L. E. Kay, A. Bax, and A. M. Gronenborn, *Biochemistry* **30,** 12 (1991).
[12] E. R. P. Zuiderweg, A. M. Petros, S. W. Fesik, and E. T. Olejniczak, *J. Am. Chem. Soc.* **113,** 370 (1991).

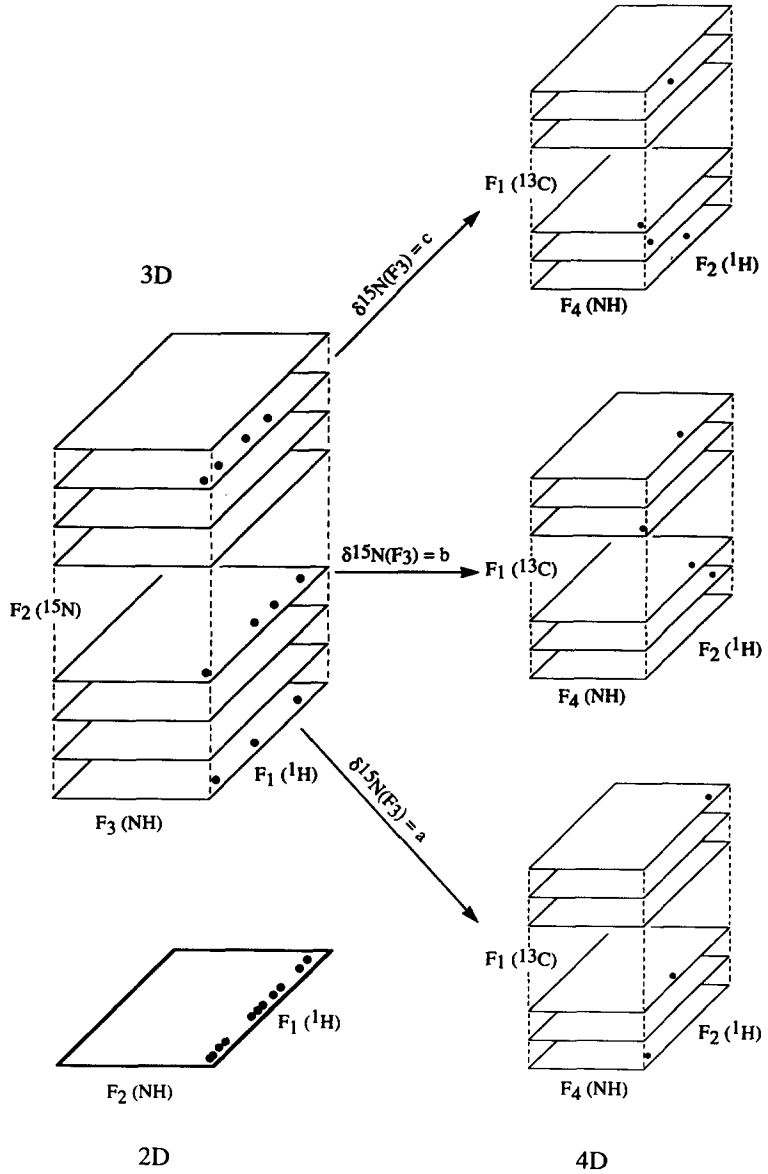

FIG. 3. Schematic illustration of the progression and relationship between 2D, 3D, and 4D heteronuclear NMR experiments. The circles represent NOE cross-peaks. In the example shown there are 11 NOEs originating from 11 different protons in the F_1 dimension to a single frequency position in the F_2 dimension. In the 2D spectrum, it is impossible to ascertain whether there is only one destination proton or several in the F_2 dimension. By spreading the spectrum into a third dimension (labeled F_2), according to the chemical shift of the

tions gives rise to the NOE. By spreading the spectrum into a third dimension, for example, by the chemical shift of the ^{15}N atoms attached to the NH protons, the number of possibilities will be reduced to two, provided, of course, that the chemical shifts of the two nitrogen atoms are different. Finally, when the fourth dimension corresponding to the chemical shift of the ^{13}C atoms attached to the aliphatic protons is introduced, a unique assignment of the NH–aliphatic proton pair giving rise to the NOE can be made.

Figure 4A presents a portion of the 2D ^{15}N-edited NOESY spectrum of interleukin 1β (153 residues) illustrating NOE interactions between the NH protons along the F_2 axis and the $C^{\alpha}H$ protons along the F_1 dimension.[11] Despite the fact that a large number of cross-peaks can be resolved, it can be seen that many of the cross-peaks have identical chemical shifts in one or other dimensions. For example, there are 15 cross-peaks involving NH protons at a F_2 (^1H) chemical shift of approximately 9.2 ppm. A single $^1H(F_1)$–$^1H(F_3)$ plane of the 3D ^{15}N-edited NOESY spectrum of interleukin 1β at $\delta^{15}N(F_2) = 123.7$ ppm is shown in Fig. 4B. Not only is the number of cross-peaks in this slice small, but at $\delta^1H(F_3) \approx 9.2$ ppm there is only a single cross-peak involving one NH proton. The correlations observed in the ^{15}N-edited NOESY spectrum are through-space ones. Intraresidue correlations from the NH protons to the $C^{\alpha}H$ and $C^{\beta}H$ protons can similarly be resolved using a 3D ^{15}N-edited HOHAHA spectrum in which efficient isotropic mixing sequences are used to transfer magnetization between protons via three-bond ^1H–^1H couplings.

The 3D ^{15}N-edited NOESY and HOHAHA spectra constitute only one of several versions of a 3D heteronuclear-edited spectrum. Many alternative through-bond pathways can be utilized to great effect. Consider, for example, the delineation of amino acid spin systems which involves grouping those resonances which belong to the same residue. In 2D NMR, correlation experiments are used to delineate either direct or relayed connectivities via small three-bond ^1H–^1H couplings. Even for proteins of 50–60 residues, it can be difficult to delineate long-chain amino

---

heteronucleus attached to the destination proton, it can be seen that the NOEs now lie in three distinct $^1H(F_1)$–$^1H(F_3)$ planes, indicating that three different destination protons are involved. However, the ^1H chemical shifts still provide the only means of identifying the originating protons. Hence, the problem of spectral overlap still prevents the unambiguous assignment of the NOEs. By extending the dimensionality of the spectrum to four, each NOE interaction is labeled by four chemical shifts along four orthogonal axes. Thus, the NOEs in each plane of the 3D spectrum are now spread over a cube in the 4D spectrum according to the chemical shift of the heteronucleus directly attached to the originating protons. (Adapted from Kay *et al.*[10])

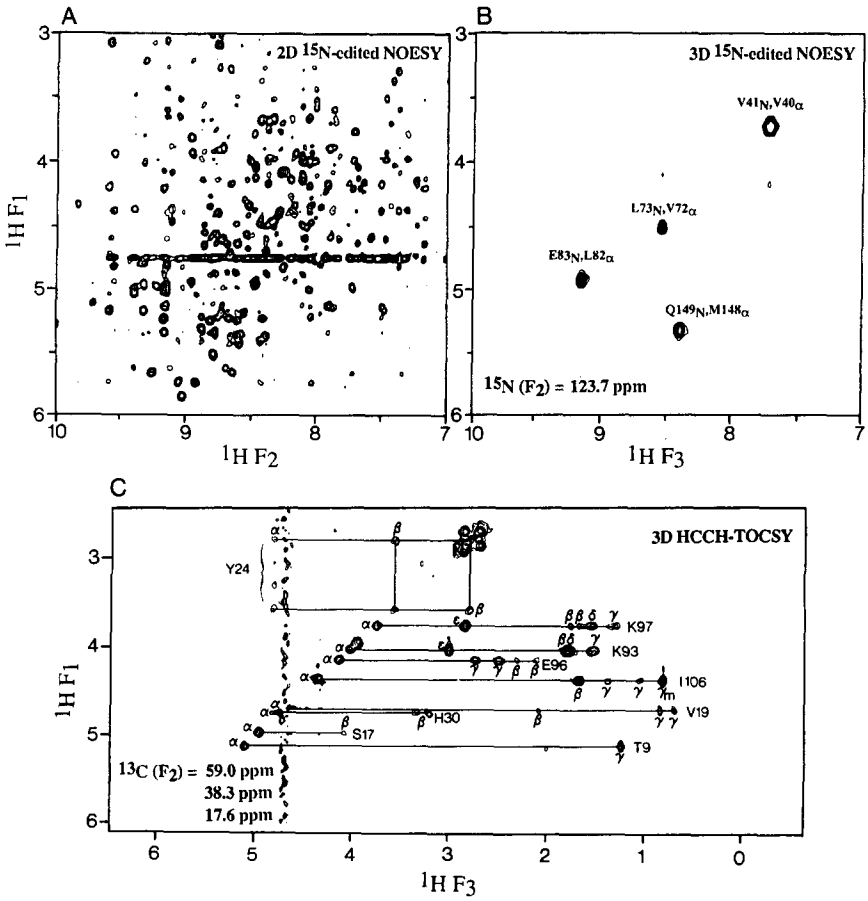

FIG. 4. Multidimensional spectra of interleukin 1β recorded at 600 MHz [G. M. Clore, A. Bax, P. C. Driscoll, P. T. Wingfield, and A. M. Gronenborn, *Biochemistry* **29,** 8172 (1990); P. C. Driscoll, G. M. Clore, D. Marion, P. T. Wingfield, and A. M. Gronenborn, *Biochemistry* **29,** 3542 (1990); P. C. Driscoll, A. M. Gronenborn, P. T. Wingfield, and G. M. Clore, *Biochemistry* **29,** 4468 (1990)]. The 2D spectrum (A) shows the NH(F_2 axis)–C$^\alpha$H(F_1 axis) region of a 2D ^{15}N-edited NOESY spectrum. The same region of a single NH(F_3)–^{1}H(F_1) plane of the 3D ^{15}N-edited NOESY at δ^{15}N(F_2) = 123.7 ppm is shown in (B). The actual 3D spectrum comprises 64 such planes, and projection of these on a single plane would yield the same spectrum as in (A). (C) Single ^{1}H(F_3)–^{1}H(F_1) plane of the 3D HCCH-TOCSY spectrum at δ^{13}C(F_2) = 38.3 $\pm$ nSW (where SW is the spectral width of 20.71 ppm in the ^{13}C dimension), illustrating both direct and relayed connectivities originating from the C$^\alpha$H protons. Note how easy it is to delineate complete spin systems of long side chains such as Lys (i.e., cross-peaks to the C$^\beta$H, C$^\gamma$H, C$^\delta$H, and C$^\epsilon$H protons are observed) owing to the fact that magnetization along the side chain is transferred via large $^1J_{CC}$ couplings. Several features of the HCCH-TOCSY spectrum should be pointed out. First, extensive folding is employed which does not obscure analysis as ^{13}C chemical shifts for different

acids such as Lys and Arg in this manner. In heteronuclear 3D NMR an alternative pathway can be employed which involves transferring magnetization first from a proton to its directly attached carbon atom via the large $^1J_{CH}$ coupling (~130 Hz), followed by either direct or relayed transfer of magnetization along the carbon chain via the $^1J_{CC}$ couplings (~30–40 Hz), before transferring the magnetization back to protons.[13,14] An example of such a spectrum is the so-called HCCH-total correlation spectroscopy (TOCSY) spectrum shown in Fig. 4C. The $^1H(F_1)$–$^1H(F_3)$ plane at $\delta^{13}C(F_2) = 59$ ppm illustrates both direct and relayed connectivities along various side chains originating from $C^\alpha H$ protons. As expected, the resolution of the spectrum is excellent, and there is no spectral overlap. Just as importantly, however, the sensitivity of the experiment is extremely high, and complete spin systems are readily identified in interleukin 1β even for long side chains, such as those of two lysine residues shown in Fig. 4C. Indeed, analyzing spectra of this kind, it was possible to obtain complete ^1H and ^{13}C assignments for the side chains of interleukin 1β[15].

Three-dimensional NMR also permits one to devise experiments for sequential assignment which are based solely on through-bond connectivities via heteronuclear couplings[8,16] and thus do not rely on the NOESY experiment. This becomes increasingly important for larger proteins, as the types of connectivities observed in these correlation experiments are entirely predictable, whereas in the NOESY spectrum, which relies solely on close proximity of protons, it may be possible to confuse sequential connectivities with long-range ones. These 3D heteronuclear correlation experiments are of the triple-resonance variety and make use of one-bond $^{13}CO(i-1)$–$^{15}N(i)$, $^{15}N(i)$–$^{13}C^\alpha(i)$, $^{13}C(i)$–$^{13}C(i)$, and $^{13}C^\alpha(i)$–$^{13}CO(i)$ couplings, as well as two-bond $^{13}C^\alpha(i-1)$–$^{15}N(i)$ couplings. In this manner

[13] A. Bax, G. M. Clore, P. C. Driscoll, A. M. Gronenborn, M. Ikura, and L. E. Kay, *J. Magn. Reson.* **87,** 620 (1990); A. Bax, G. M. Clore, and A. M. Gronenborn, *J. Magn. Reson.* **88,** 425 (1990).

[14] S. W. Fesik, H. L. Eaton, E. T. Olejniczak, E. R. P. Zuiderweg, L. P. McIntosh, and F. W. Dahlquist, *J. Am. Chem. Soc.* **112,** 886 (1990).

[15] G. M. Clore, A. Bax, P. C. Driscoll, P. T. Wingfield, and A. M. Gronenborn, *Biochemistry* **29,** 8172 (1990).

[16] M. Ikura, L. E. Kay, and A. Bax, *Biochemistry* **29,** 4659 (1990); R. Powers, A. M. Gronenborn, G. M. Clore, and A. Bax, *J. Magn. Reson.* **94,** 209 (1991).

---

carbon types are located in characteristic regions of the ^{13}C spectrum with little overlap. Second, the spectrum is edited according to the chemical shift of the heteronucleus attached to the originating proton rather than the destination one. Third, multiple cross-checks on the assignments are readily made by looking for the symmetry-related peaks in the planes corresponding to the ^{13}C chemical shifts of the destination protons in the original slice.

multiple independent pathways for linking the resonances of one residue with those of its adjacent neighbor are available, thereby avoiding ambiguities in the sequential assignment (Table I).

In practice, only a limited number of 3D triple- and double-resonance experiments need to be performed to obtain complete assignments. In our experience, the following eight 3D experiments not only provide all the information required, but are also characterized by high sensitivity and can be recorded in as little as 2 weeks of measuring time. Specifically, the 3D CBCA(CO)NH and HBHA(CBCACO)NH experiments[17] are used to correlate the chemical shifts of $C^{\alpha}(i)/C^{\beta}(i-1)$ and $H^{\alpha}(i)/H^{\beta}(i-1)$, respectively, of residue $i-1$ with the $^{15}N(i)/NH(i)$ chemical shifts of residue i; the complementary 3D C(CO)NH and H(CCO)NH experiments[18] are used to correlate the chemical shifts of the aliphatic side-chain ^{13}C and ^{1}H resonances, respectively, of residue $i-1$ with the $^{15}N(i)/NH(i)$ chemical shifts of residue i. In the first two experiments, magnetization originating on C^{β} is transferred to C^{α} by a COSY mixing pulse, whereas in the second pair of experiments, magnetization is transferred from a side-chain C along the carbon chain to C^{α} via isotropic mixing. Intraresidue correlations to the NH group can be obtained from the 3D CBCANH[19] and ^{15}N-edited HOHAHA[20] experiments. The 3D CBCANH experiment correlates the chemical shifts of $C^{\alpha}(i)/C^{\beta}(i)$ [as well as those of $C^{\alpha}(i-1)/C^{\beta}(i-1)$ which invariably give rise to weaker cross-peaks] with the $^{15}N(i)/NH(i)$ chemical shifts of residue i; the 3D ^{15}N-separated HOHAHA experiment correlates the chemical shifts of the side-chain protons of residue i with the $^{15}N(i)/NH(i)$ chemical shifts of residue i. Finally, the 3D HCCH-COSY and HCCH-TOCSY experiments[13] can be used to confirm and obtain complete ^{1}H and ^{13}C assignments of the side chains (Table I).

The power of 4D heteronuclear NMR spectroscopy for unraveling interactions that would not have been possible in lower dimensional spectra is illustrated in Fig. 5 by the $^{13}C/^{13}C$-edited NOESY spectrum of interleukin 1β.[11] Figure 5A shows a small portion of the aliphatic region between 1 and 2 ppm of a conventional 2D NOESY spectrum of interleukin 1β. The overlap is so great that no single individual cross-peak can be resolved. One might therefore wonder just how many NOE interactions are actually superimposed, for example, at the ^{1}H chemical shift coordinates of the letter X at 1.39 (F_1) and 1.67 (F_2) ppm. A $^{1}H(F_2)$–$^{1}H(F_4)$

[17] S. Grzesiek and A. Bax, *J. Am. Chem. Soc.* **114,** 6291 (1992); S. Grzesiek and A. Bax, *J. Biomol. NMR* **3,** 185 (1993).
[18] S. Grzesiek, J. Anglister, and A. Bax, *J. Magn. Reson.* in press (1993).
[19] S. Grzesiek and A. Bax, *J. Magn. Reson.* **99,** 201 (1992).
[20] G. M. Clore, A. Bax, and A. M. Gronenborn, *J. Biomol. NMR* **11,** 13 (1991).

TABLE I
CORRELATIONS OBSERVED IN THREE-DIMENSIONAL DOUBLE- AND TRIPLE-RESONANCE EXPERIMENTS USED FOR SEQUENTIAL AND SIDE-CHAIN ASSIGNMENTS

Experiment	Correlation	J Coupling[a]
^{15}N-edited HOHAHA	$C^{\alpha}H(i)$–$^{15}N(i)$–$NH(i)$	$^{3}J_{HN^{\alpha}}$ (~3–11 Hz)
	$C^{\beta}H(i)$–$^{15}N(i)$–$NH(i)$	$^{3}J_{HN^{\alpha}}$ (~3–11 Hz), $^{3}J_{\alpha\beta}$ (~3–11 Hz)
H(CA)NH	$C^{\alpha}H(i)$–$^{15}N(i)$–$NH(i)$	$^{1}J_{NC^{\alpha}}$ (~9–13 Hz)
	$C^{\alpha}H(i-1)$–$^{15}N(i)$–$NH(i)$	$^{2}J_{NC^{\alpha}}$ (~5–10 Hz)
HN(CO)HB	$C^{\alpha}H(i-1)$–$^{15}N(i)$–$NH(i)$	$^{2}J_{COH^{\alpha}}$ (~4–7 Hz)
	$C^{\beta}H(i-1)$–$^{15}N(i)$–$NH(i)$	$^{3}J_{COH^{\beta}}$ (~8 Hz for trans coupling)
HNHB	$C^{\beta}H(i)$–$^{15}N(i)$–$NH(i)$	$^{3}J_{NH^{\beta}}$ (~5 Hz for trans coupling)
HNCA	$^{13}C^{\alpha}(i)$–$^{15}N(i)$–$NH(i)$	$^{1}J_{NC^{\alpha}}$ (~9–13 Hz)
	$^{13}C^{\alpha}(i-1)$–$^{15}N(i)$–$NH(i)$	$^{2}J_{NC^{\alpha}}$ (~5–10 Hz)
CBCANH	$^{13}C^{\beta}/C^{\alpha}(i)$–$^{15}N(i)$–$NH(i)$	$^{1}J_{CC}$ (~30–40 Hz), $^{1}J_{NC^{\alpha}}$ (~9–13 Hz)
	$^{13}C^{\beta}/C^{\alpha}(i-1)$–$^{15}N(i)$–$NH(i)$	$^{1}J_{CC}$ (~30–40 Hz), $^{2}J_{NC^{\alpha}}$ (~5–10 Hz)
HN(CO)CA	$^{13}C^{\alpha}(i-1)$–$^{15}N(i)$–$NH(i)$	$^{1}J_{NCO}$ (~15 Hz), $^{1}J_{C^{\alpha}CO}$ (~55 Hz)
CBCA(CO)NH	$^{13}C^{\beta}/C^{\alpha}(i-1)$–$^{15}N(i)$–$NH(i)$	$^{1}J_{CC}$ (~30–40 Hz), $^{1}J_{NCO}$ (~15 Hz), $^{1}J_{C^{\alpha}CO}$ (~55 Hz)
HBHA(CBCACO)NH	$C^{\beta}H/C^{\alpha}H(i-1)$–$^{15}N(i)$–$NH(i)$	$^{1}J_{CC}$ (~30–40 Hz), $^{1}J_{NCO}$ (~15 Hz), $^{1}J_{C^{\alpha}CO}$ (~55 Hz)
C(CO)NH	$^{13}C^{x}(i-1)$–$^{15}N(i)$–$NH(i)$	$^{1}J_{CC}$ (~30–40 Hz), $^{1}J_{NCO}$ (~15 Hz), $^{1}J_{C^{\alpha}CO}$ (~55 Hz)
H(CCO)NH	$C^{x}H(i-1)$–$^{15}N(i)$–$NH(i)$	$^{1}J_{CC}$ (~30–40 Hz), $^{1}J_{NCO}$ (~15 Hz), $^{1}J_{C^{\alpha}CO}$ (~55 Hz)
HNCO	$^{13}CO(i-1)$–$^{15}N(i)$–$NH(i)$	$^{1}J_{NCO}$ (~15 Hz)
HCACO	$C^{\alpha}H(i)$–$^{13}C^{\alpha}(i)$–$^{13}CO(i)$	$^{1}J_{C^{\alpha}CO}$ (~55 Hz)
HCA(CO)N	$C^{\alpha}H(i)$–$^{13}C^{\alpha}(i)$–$^{15}N(i+1)$	$^{1}J_{C^{\alpha}CO}$ (~55 Hz), $^{1}J_{NCO}$ (~15 Hz)
HCCH-COSY	$H(j)$–$^{13}C(j)$–$^{13}C(j \pm 1)$–$H(j \pm 1)$	$^{1}J_{CC}$ (~30–40 Hz)
HCCH-TOCSY	$H(j)$–$^{13}C(j) \ldots {}^{13}C(j \pm n)$–$H(j \pm n)$	$^{1}J_{CC}$ (~30–40 Hz)

[a] In addition to the couplings indicated, all experiments make use of the $^{1}J_{CH}$ (~140 Hz) and/or $^{1}J_{NH}$ (~95 Hz) couplings.

plane of the 4D spectrum at $\delta^{13}C(F_1)$, $\delta^{13}C(F_3)$ = 44.3, 34.6 ppm is shown in Fig. 5B, and the square box at the top right-hand side of Fig. 5B encloses the region between 1 and 2 ppm. Only two cross-peaks are present in this region, and the arrow points to a single NOE between the $C^{\gamma}H$ and $C^{\beta}H$ protons of Lys-77 with the same ^{1}H chemical shift coordinates as X in Fig. 5A. All other NOE interactions at the same ^{1}H chemical shift coordinates can be determined by inspection of a single $^{13}C(F_1)$–$^{13}C(F_3)$ plane taken at $\delta^{1}H(F_2)$, $\delta^{1}H(F_4)$ = 1.39, 1.67 ppm. This reveals a total of seven NOE interactions superimposed at the ^{1}H chemical shift coordinates of X.

Another feature of the 4D spectrum is illustrated by the two $^{1}H(F_2)$–$^{1}H(F_4)$ planes at different F_1 and F_3 ^{13}C frequencies shown in

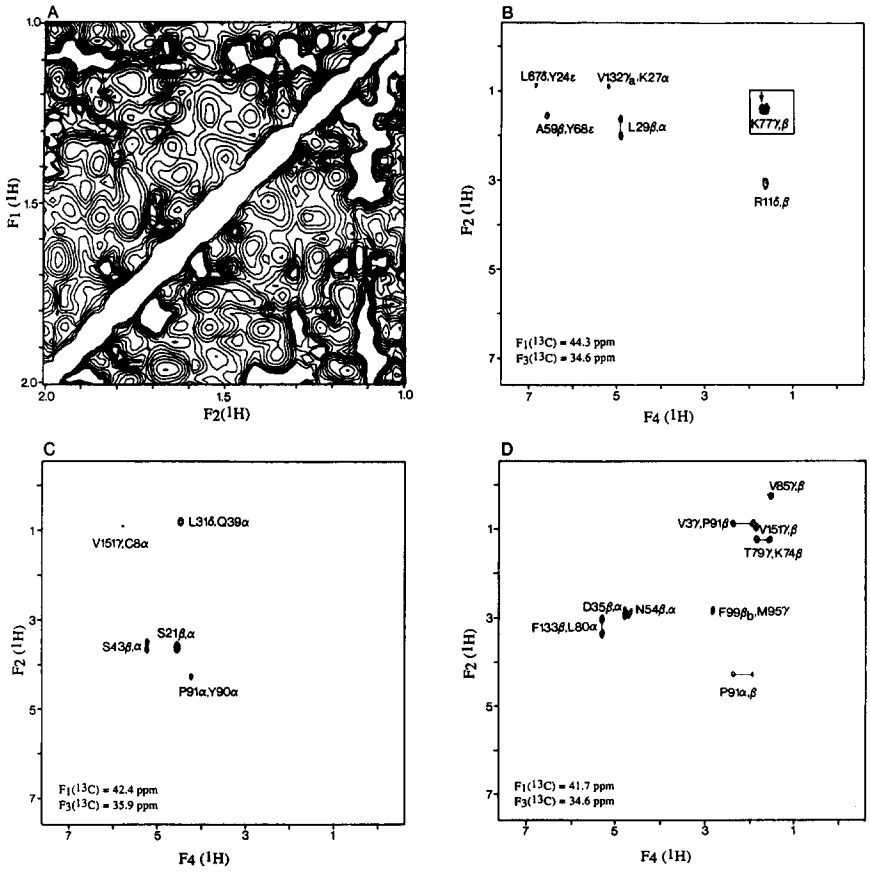

FIG. 5. Comparison of 2D and 4D NMR spectra of interleukin 1β recorded at 600 MHz.[11] The region between 1 and 2 ppm of the 2D NOESY spectrum is shown in (A). $^1H(F_2)$–$^1H(F_4)$ planes at several $^{13}C(F_1)$ and $^{13}C(F_3)$ frequencies of the 4D $^{13}C/^{13}C$ NOESY spectrum are shown in (B)–(D). No individual cross-peaks can be observed in the 2D spectrum, and the letter X has ^1H coordinates of 1.39 and 1.67 ppm. In contrast, only two cross-peaks are observed in the boxed region in (B) between 1 and 2 ppm, one of which (indicated by an arrow) has the same ^1H coordinates as X. Further analysis of the complete 4D spectrum reveals the presence of seven NOE cross-peaks superimposed at the ^1H coordinates of X. This can be ascertained by looking at the $^{13}C(F_1)$–$^{13}C(F_3)$ plane taken at the ^1H coordinates of X. True diagonal peaks corresponding to magnetization that has not been transferred from one proton to another, as well as intense NOE peaks involving protons attached to the same carbon atom (i.e., methylene protons), appear in only a single $^1H(F_2)$–$^1H(F_4)$ plane of each $^{13}C(F_1)$, $^1H(F_2)$, $^1H(F_4)$ cube at the carbon frequency where the originating and destination carbon atoms coincide (i.e., at $F_1 = F_3$). Thus, these intense resonances no longer obscure NOEs between protons with similar or degenerate chemical shifts. Two examples of such NOEs can be seen in (C) (between the $C^\alpha H$ protons of Pro-91 and Tyr-90) and (D) (between one of the $C^\beta H$ protons of Phe-99 and the methyl protons of Met-95).

Fig. 5C,B. In both cases, there are cross-peaks involving protons with identical or near chemical shifts, namely, that between Pro-91($C^{\alpha}H$) and Tyr-90($C^{\alpha}H$), diagnostic of a *cis*-proline, in Fig. 5C, and between Phe-99($C^{\beta b}H$) and Met-95($C^{\gamma}H$) in Fig. 5D. These interactions could not be resolved in either a 2D spectrum or a 3D ^{13}C-edited spectrum as they would lie on the spectral diagonal (i.e., the region of the spectrum corresponding to magnetization that has not been transferred from one proton to another). In the 4D spectrum, however, they are easy to observe, provided, of course, that the ^{13}C chemical shifts of the directly bonded ^{13}C nuclei are different.

Because the number of NOE interactions present in each $^1H(F_4)$–$^1H(F_2)$ plane of 4D $^{13}C/^{15}N$- or $^{13}C/^{13}C$-edited NOESY spectra is so small, the inherent resolution in a 4D spectrum is extremely high, despite the low level of digitization. Indeed, spectra with equivalent resolution can be recorded at magnetic field strengths considerably lower than 600 MHz,

---

These various planes of the 4D spectrum also illustrate another key aspect of 3D and 4D NMR, namely, the importance of designing the optimal pulse scheme to remove undesired artifacts which may severely interfere with the interpretation of the spectra. Thus, whereas the 4D $^{13}C/^{13}C$-edited NOESY experiment is conceptually analogous to that of a 4D $^{13}C/^{15}N$-edited one, the design of a suitable pulse scheme is actually much more complex in the $^{13}C/^{13}C$ case. This is due to the fact that there are a large number of spurious magnetization transfer pathways that can lead to observable signals in the homonuclear $^{13}C/^{13}C$ case. For example, in the 4D $^{15}N/^{13}C$-edited case there are no "diagonal peaks" which would correspond to magnetization that has not been transferred from one hydrogen to another, as the double heteronuclear filtering (i.e., ^{13}C and ^{15}N) is extremely efficient at completely removing these normally very intense and uninformative resonances. Such a double filter is not available in the $^{13}C/^{13}C$ case so that both additional pulses and phase cycling are required to suppress magnetization transfer through these pathways. This task is far from trivial, as the number of phase cycling steps in 4D experiments is severely limited by the need to keep the measurement time down to practical levels (i.e., less than 1 week). The most efficient way of obtaining artifact-free spectra is through the incorporation of pulsed-field gradients to suppress undesired coherence transfer pathways [A. Bax and S. S. Pochapsky, *J. Magn. Reson.* **99,** 638 (1992)]. Indeed, inclusion of six pulsed-field gradients into the original pulse scheme of Clore *et al.*[11] reduces the phase cycle from eight to two steps [G. W. Vuister, G. M. Clore, A. M. Gronenborn, R. Powers, D. S. Garrett, R. Tschudin, and A. Bax, *J. Magn. Reson. Ser. B* **101,** 210 (1993)]. The results of such care in pulse design can be clearly appreciated from the artifact-free planes shown in (B)–(D). However, when a 4D $^{13}C/^{13}C$-edited NOESY spectrum is recorded with the same pulse scheme as that used in the 4D $^{15}N/^{13}C$ experiment (with the obvious replacement of ^{15}N pulses by ^{13}C pulses), a large number of spurious peaks are observed along a pseudodiagonal at $\delta^1H(F_2) = \delta^1H(F_4)$ in planes where the carbon frequencies of the originating and destination protons do not coincide. As a result, it becomes virtually impossible under these circumstances to distinguish artifacts from NOEs between protons with the same ^1H chemical shifts, as was possible with complete confidence in (C) and (D).

although this would obviously lead to a reduction in sensitivity. Further, it can be calculated that 4D spectra with virtual lack of resonance overlap and good sensitivity can be obtained on proteins with as many as 400 residues. Thus, once complete ^{1}H, ^{15}N, and ^{13}C assignments are obtained, analysis of 4D spectra should permit the automated assignment of almost all NOE interactions.

Conclusion

In this chapter we have summarized developments in heteronuclear 3D and 4D NMR studies designed to extend the NMR methodology to medium-sized proteins in the range 15–30 kDa. The underlying principle of this approach consists of extending the dimensionality of the spectra to obtain dramatic improvements in spectral resolution while simultaneously exploiting large heteronuclear couplings to circumvent problems associated with larger line widths. A key feature of all the experiments is that they do not result in any increase in the number of observed cross-peaks relative to the 2D counterparts. Hence, the improvement in resolution is achieved without raising the spectral complexity, rendering data interpretation straightforward. Thus, for example, in 4D heteronuclear-edited NOESY spectra, the NOE interactions between proton pairs are labeled not only by the ^{1}H chemical shifts but also by the corresponding chemical shifts of their directly bonded heteronuclei in four orthogonal axes of the spectrum. Also important in terms of practical applications is the high sensitivity of these experiments, which makes it feasible to obtain high-quality spectra in a relatively short time frame on 1–2 m*M* protein samples uniformly labeled with ^{15}N and/or ^{13}C.

Just as 2D NMR permitted the application of NMR to the structure determination of small proteins of less than about 100 residues, 3D and 4D heteronuclear NMR provide the means of extending the methodology to medium-sized proteins in the range of 150 to 300 residues. Indeed, the determination in 1991 of the first high-resolution structure of a protein in the 15–20 kDa range, namely, the cytokine interleukin 1β (153 residues and 18 kDa), using 3D and 4D heteronuclear NMR[21] demonstrated beyond doubt that the technology is now available for obtaining the structures of such medium-sized proteins at a level of accuracy and precision comparable to the best results attainable for small proteins. Subsequently, a number of other medium-sized protein structures have been determined

[21] G. M. Clore, P. T. Wingfield, and A. M. Gronenborn, *Biochemistry* **30,** 2315 (1991).

using these methods, including those of interleukin 4,[22] a complex of calmodulin with a target peptide,[23] and a complex of cyclophilin and cyclosporin A.[24]

Acknowledgments

We thank Ad Bax for many stimulating discussions. This work was supported in part by the AIDS Targeted Anti-Viral Program of the Office of the Director of the National Institutes of Health. This chapter has been adapted and updated from G. M. Clore and A. M. Gronenborn, *Science* **252,** 1390 (1991).

[22] R. Power, D. S. Garrett, C. J. March, E. A. Frieden, A. M. Gronenborn, and G. M. Clore, *Science* **256,** 1673 (1992); L. J. Smith, C. Redfield, J. Boyd, G. M. P. Lawrence, R. G. Edwards, R. A. G. Smith, and C. M. Dobson, *J. Mol. Biol.* **224,** 899 (1992); R. Power, D. S. Garrett, C. J. March, E. A. Frieden, A. M. Gronenborn, and G. M. Clore, *Biochemistry* **32,** 6744 (1993).

[23] M. Ikura, G. M. Clore, A. M. Gronenborn, G. Zhu, C. B. Klee, and A. Bax, *Science* **256,** 632 (1992).

[24] Y. Thierault, T. M. Logan, R. Meadows, L. Yu, E. T. Olejniczak, T. F. Holzman, R. L. Simmer, and S. W. Fesik, *Nature (London)* **361,** 88 (1993).

[12] Chemical Shifts as a Tool for Structure Determination

By DAVID S. WISHART and BRIAN D. SYKES

Introduction

Chemical shifts are the most accessible quantities in nuclear magnetic resonance (NMR) spectroscopy. Because of their ease of measurement and the accuracy with which they can be determined, it has long been believed that chemical shifts could eventually offer the richest source of information to spectroscopists wishing to learn more about the detailed structure of proteins. Attempts to mine this tremendous source of information began in the mid to late 1960s with the landmark helix–coil studies of Jardetzky and co-workers[1] and the theoretical developments of Sternlicht and Wilson[2] and, later, Tigelaar and Flygare.[3] These early workers, along with many other later contributors,[4–6] attempted to relate so-called

[1] J. L. Markley, D. H. Meadows, and O. Jardetzky, *J. Mol. Biol.* **27,** 25 (1967).
[2] H. Sternlicht and D. Wilson, *Biochemistry* **6,** 2881 (1967).
[3] H. L. Tigelaar and W. H. Flygare, *J. Am. Chem. Soc.* **94,** 343 (1972).
[4] N. J. Clayden and R. J. P. Williams, *J. Magn. Reson.* **49,** 383 (1982).
[5] A. Pardi, G. Wagner, and K. Wüthrich, *Eur. J. Biochem.* **137,** 454 (1983).
[6] D. C. Dalgarno, B. A. Levine, and R. J. P. Williams, *Biosci. Rep.* **3,** 443 (1983).